

See discussions, stats, and author profiles for this publication at: <https://www.researchgate.net/publication/357588700>

Stratigraphic Characterization of the Eagle Ford Shale to Identify the Best Landing Zone: A Semi-analytical Workflow

Article in *Interpretation* · January 2022

DOI: 10.1190/int-2021-0111.1

CITATIONS

0

READS

775

3 authors, including:



Ajit Kumar Sahoo

Saudi Aramco

18 PUBLICATIONS 280 CITATIONS

[SEE PROFILE](#)



Vikram Vishal

Indian Institute of Technology Bombay

117 PUBLICATIONS 3,568 CITATIONS

[SEE PROFILE](#)

Stratigraphic characterization of the Eagle Ford shale to identify the best landing zone: A semianalytical workflow

Ajit K. Sahoo¹, Vikram Vishal¹, and Mukul Srivastava²

Abstract

Placement of the horizontal well within the best landing zone is critical to maximize well productivity; thus, identification of the best landing zone is important. This paper illustrated an integrated semianalytical workflow to carry out the stratigraphic characterization of the Eagle Ford shale to identify the best landing zone. The objective of this work is twofold: (1) to establish a workflow for stratigraphic characterization and (2) to understand the local level variability in the well performance. To establish the workflow, we have used the production data, petrophysical information, and regional reservoir property maps. As a first step of the workflow, we subdivided the Eagle Ford shale into nine smaller stratigraphic units using the wireline signatures and outcrop study. In the second step, we have used statistical methods such as linear regression, fuzzy groups, and theory of granularity to capture the relationship between the geologic parameters and the well performances. In this step, we identified volume of clay (Vclay), hydrocarbon filled porosity (HCFP), and total organic carbon (TOC) as key drivers of the well performance. In the third step, we characterized the nine smaller units and identified four stratigraphic units as good reservoirs with two being the best due to their low Vclay: high HCFP and high TOC content. Finally, we reviewed the well paths of four horizontal wells with respect to the best stratigraphic units. We observed that the production behavior of these wells was possibly driven by their lateral placement. The better producing wells were placed within the middle of the best stratigraphic units, whereas the poor wells were going out the best stratigraphic units. This investigation provided a case study that demonstrated the importance of integrating data sets to identify best landing zones, and the suggested workflow could be applied to other areas and reservoirs to better identify targetable zones.

Introduction

It is critical to understand that shale reservoirs are heterogeneous and parameters such as porosity, permeability, and organic richness, brittleness along with engineering development strategies such as proppant type, proppant volume, stage spacing, and cluster spacing, have significant bearing on well performance. In addition to the above parameters, effective lateral placement within the best part of the reservoir is critical to maximize well productivity. The precision in placement of the wellbore vertically or “landed” laterally is critical to optimum stimulation, fracture geometry, and the resultant well production. There are many theories in the industry about the zone of interest where the lateral should be horizontally drilled, but the standard convention is to target the best quality rock with consideration given to the stress profile. The success of a well depends on the selection of well-placement targets that will help to generate optimum reservoir coverage through effective hydraulic fracturing, ultimately, leading to better

production performance (Cipolla et al., 2008; Sahoo Ajit et al., 2013, 2014, 2018; Algarhy et al., 2015; Sahoo et al., 2015; Stephenson et al., 2015; Gupta et al., 2016; Dutta et al., 2018, 2019; Urban-Rascon et al., 2018; Hazra et al., 2018a, 2018b; Vishal et al., 2019).

Eagle Ford is one of the major producing shales play of North America. In this paper, we characterize the local level heterogeneity observed within the study area of the Eagle Ford shale through stratigraphic characterization. We also establish a semianalytical workflow to carry out the stratigraphic characterization of the Eagle Ford shale. This stratigraphic characterization is carried out to understand the reasons behind the different production behavior of two closely drilled horizontal wells. The horizontal distance between the laterals of the two wells is 1000 ft. This case study demonstrates the importance of integrating data sets to identify best landing zones, and the suggested workflow can be applied to other areas of this play and other shale reservoirs around the globe to better identify targetable zones.

¹IIT Bombay, Department of Earth Sciences, Computation and Experimental Geomechanics Laboratory, Mumbai 400076, India. E-mail: ajitsahoo.iitb@gmail.com (corresponding author); v.vishal@iitb.ac.in.

²Reliance Industries Ltd., E&P Business, Navi, Mumbai 400701, India. E-mail: mukulwins@gmail.com.

Manuscript received by the Editor 23 May 2021; revised manuscript received 1 December 2021; published ahead of production 4 January 2022; published online 14 March 2022. This paper appears in *Interpretation*, Vol. 10, No. 2 (May 2022); p. T305–T323, 21 FIGS., 7 TABLES.
http://dx.doi.org/10.1190/INT-2021-0111.1. © 2022 Society of Exploration Geophysicists and American Association of Petroleum Geologists

Eagle Ford shale and its development history

The Eagle Ford shale is an Upper Cretaceous shale formation that acts as a prolific source rock for many conventional reservoirs in the Gulf of Mexico basin. This shale play covers the southwest area of Texas (Figure 1a). The Eagle Ford shale is primarily an organic-rich fossiliferous marine shales and marls with interbedded thin limestones (Surles, 1987).

The Eagle Ford Formation stratigraphically lies above Buda Limestone and below Austin Chalk. The Eagle Ford-Buda contact is a regional unconformity (Figure 1b). The entire Eagle Ford is grossly divided into upper and lower units. The upper unit is less organic-rich, whereas the lower unit is rich in organic content. The underlying Buda Limestone is mechanically very strong and acts as a frac barrier, which prohibits the hydraulic fracture not to grow downward and keep them inside the reservoir zone (White et al., 2001; Hentz and Ruppel, 2011; Workman, 2013). The Eagle Ford shale is rich in carbonate, which makes it brittle and easy to be hydraulically fractured.

Petrohawk Energy Corporation started exploration activity in the Eagle Ford shale in 2008 by drilling a wildcat well in LaSalle County and discovered the Hawkvile field. After that the boundaries of the Eagle Ford shale play continuously expanded with further discoveries. The current Eagle Ford boundaries cover an area of approximately 50,000 km². All forms of hydrocarbon (dry gas, wet gas, condensate, light oil, and black oil) are generated within the Eagle Ford depending on its thermal maturity (VRo) and depth of occurrence. Due to its different hydrocarbon type and favorable brittleness, drilling activity increased and the production has reached its peak rate in 2015 with 1,188,418 barrels of oil and 6079 million cubic feet of gas per day. As a result of the crash in oil price in

late 2014, production decreased, and currently, the Eagle Ford shale is producing approximately 1,100,000 barrels of oil and 6 billion cubic feet of gas per day (U.S. Energy Information Administration, 2021).

Problem statement

On reviewing the normalized production (normalized by dividing the cumulative production with the lateral length) of the wells falling within the study area, it is observed that the two wells (5A and 5B) shown in Figure 2 are drastically different in their performances. The horizontal spacing between the laterals of wells 5A and 5B is 1000 ft and vertically drilled through lower Eagle Ford zone. Because both the wells are drilled very close to each other and drilled through the same lower Eagle Ford, the reservoir properties of the entire lower Eagle Ford are expected to be within similar ranges (Table 1). The completion design and choke size of both the wells also are similar (Table 1). Despite of similarity reservoir qualities, completion design, and choke size, the normalized productions of both the wells are quite different. The normalized 12 month cumulative production of well 5A is 262 million cubic feet equivalent (MMCFE), whereas well 5B has produced 418 MMCFE. This inconsistent production behavior cannot be attributed to any geologic heterogeneity within 1000 ft apart. There could be other reasons such as major fault, interference, depletion, well bashing, and well sequencing behind the inconsistent production behavior of these two nearby wells. We have observed subseismic faults along both these wells. If the fault was there in the poor producing well 5A only and not in the better producing well 5B, then we could have suspected that the poor production in well 5A may be because of fault. These two wells are primary one-off wells drilled during the early phase of the development

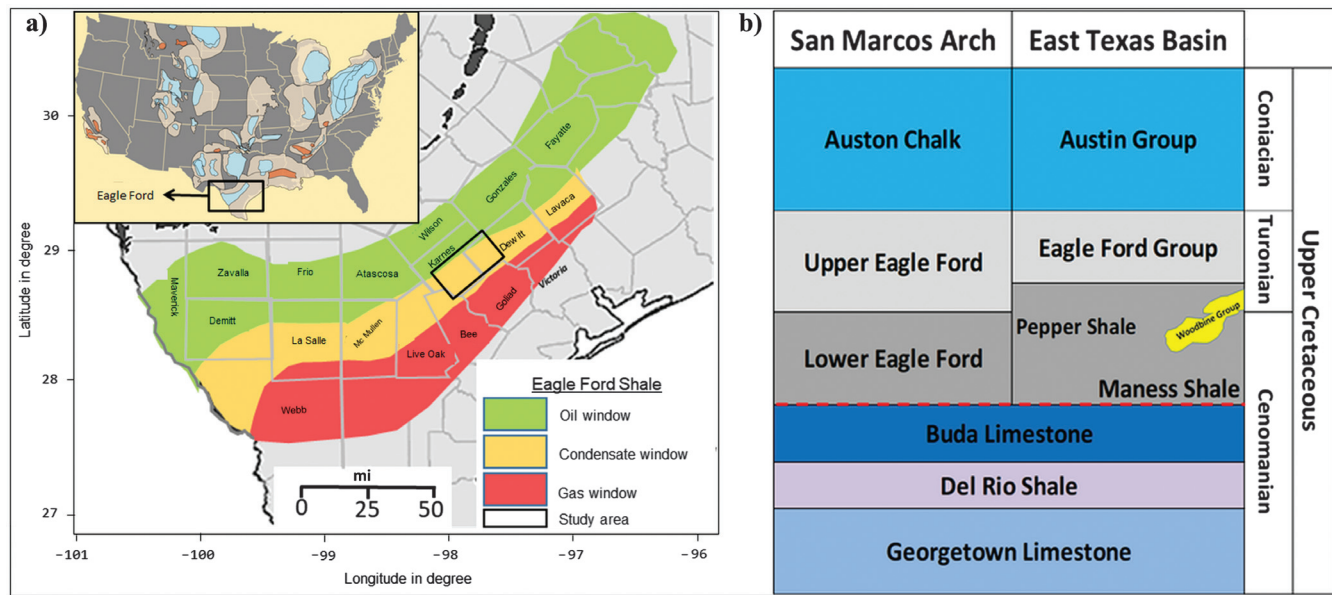


Figure 1. (a) Location and extension of the Eagle Ford shale showing study area within the black rectangle. (b) General stratigraphy of the Eagle Ford shale.

within a virgin reservoir. Therefore, there is rarely any chance of drilling these wells within a depleted reservoir. The wells are 1000 ft apart and drilled and completed within one month, so the well interference and well sequencing may not be affecting their production. Thus, we decided to review these two wells from the lateral placement point of view with regard to the best landing point. These two wells were drilled vertically within the same zone, i.e., lower Eagle Ford which is 120–200 ft thick. In this study, an attempt was made to identify the best landing zone through stratigraphic characterization and review their lateral placement in a finer scale. It has been observed in Marcellus that the wells placed within best landing zone (zone of high organic content and high silica) have given better production rates in comparison with others (David et al., 2010; Gupta et al., 2016). Eagle Ford shale (Figure 3b and 3c) being different from Marcellus, identification of the best landing zone from the raw wireline log was a challenge. In shale plays like Marcellus, the best target zone is commonly chosen based on the highest gamma-ray reading [above 250 American Petroleum Institute (API)] (Figure 3a; Gupta et al., 2016; Slatt Roger et al., 2018; Smyer et al., 2019). In the study area of Eagle Ford, we could not observe such similar high gamma-ray log signature to demarcate the best landing zone (Figure 3b). We have checked the gamma signature on a different scale (0–150) (Figure 3c) to see if there is any high gamma zone within Eagle Ford that can be considered as best landing zone. We found few high gamma zones, but those are not that typical like Marcellus which is due to very high total organic carbon (TOC) (Figure 3c). Many operators such as Marathon Oil

and Pioneer Natural Resources have used the wireline logs and chemostratigraphic approach to identify the best landing zone and described the importance of placing the lateral within that zone (Grammar and Workman, 2013; Tinnin et al., 2013; Meyer, 2018). In this paper, we

Table 1. Gross geologic parameters and key completion parameters of wells 5A and 5B.

Parameters	Well 5A	Well 5B
Gross geologic parameters for Eagle Ford		
Depth (true vertical depth sub-Sea-ft)	12,550	12,600
Gross thickness (ft)	230	238
TOC (wt%)	4.2	4.2
HCFP (%)	7.9	8.1
Vclay (%)	17	18
Completion parameters		
Stage spacing (ft)	420	420
Cluster spacing (ft)	70	70
Proppant type	Ceramic (40/80 hydroprop)	Ceramic (40/80 hydroprop)
Proppant volume (lbs/ft)	1220	1222
Average barrels per minute (BPM)	70	70
Fluid volume (bbl/ft)	19.9	19.8
Fluid type	Hybrid gel	Hybrid gel
Choke size	12/64 in	12/64 in

Both the wells have similar geology, completion design, and choke size.

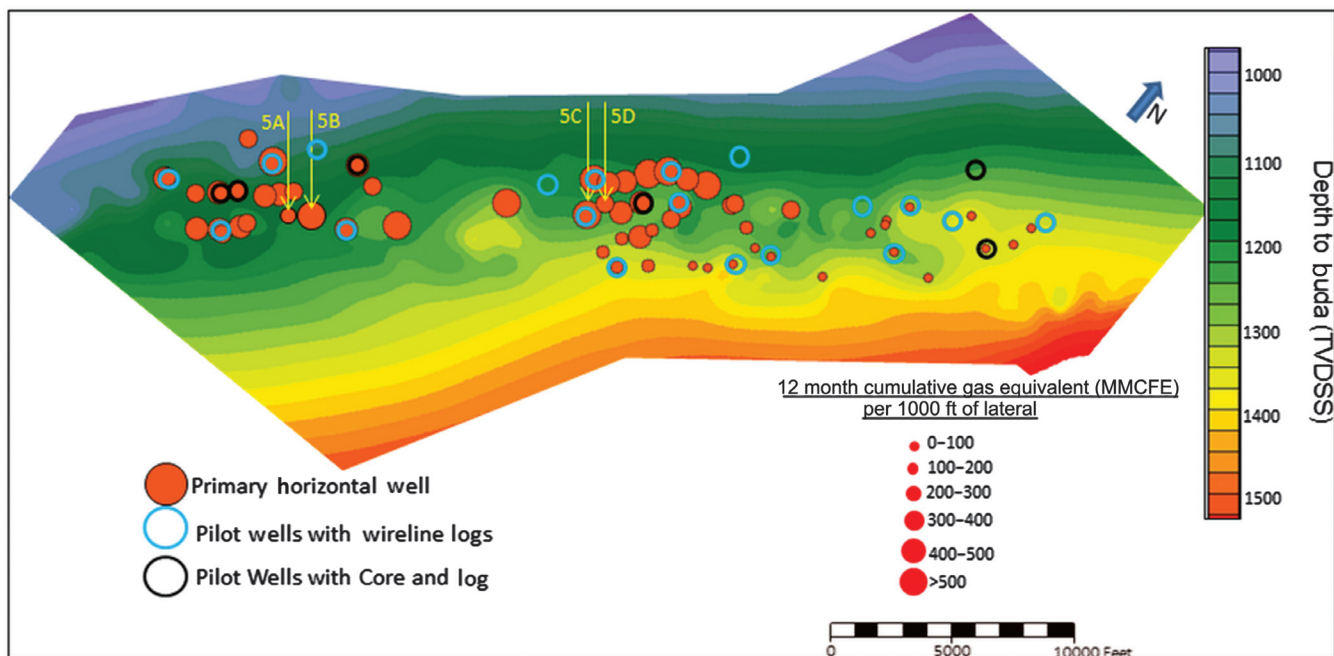


Figure 2. Local level heterogeneity in well performance between wells 5A and 5B. Both the wells are approximately 1000 ft away from each other. First 12 month normalized production (MMCFE/1000 ft) of well 5B is better than well 5A. The pilot wells with wireline logs are shown with the blue circles. The wells with core PHIT, SWT, TOC, and X-ray diffraction analysis (XRD) measurements and wireline logs are shown with the black circles.

have attempted an integrated approach of stratigraphic characterization to identify the best landing zone.

Importance of effective lateral placement

To understand the importance of lateral placement, it is necessary to determine the effectiveness of the hydraulic fracturing. The effectiveness of hydraulic fracturing depends on the geomechanical character of the shale reservoir, frac barrier, proppant volume, and fluid injection rates. Higher brittleness, higher volume

of proppant, fluid and better injection rate usually generate complex fracture network and more stimulated rock volume, which leads to better production (Lucas et al., 2010; Thomson et al., 2016).

The vertical and lateral extent of the fractures has been evaluated through multiple methods such as microseismic, fracture modeling, pressure interference test, and tracer surveys within the Eagle Ford (Zillur and Al-Qahtan, 2001; Eslinger, 2007; Kampfer and Dawson, 2016; Roussel and Agrawal, 2017; Urban-Rascon et al., 2018; El Sgher et al., 2021). Raterman et al. (2017) studied core, cuttings samples, borehole-image logs, tracer logs, microseismic, distributed temperature sensing/distributed acoustic sensing, and pressure data after hydraulic fracturing to understand the spatial distribution of proppant around the wellbore. They indicated that the maximum distribution of proppant is limited to the well bore, and it decreases as we move away (Raterman et al., 2017).

Because we have no such high-quality data sets, we have reviewed the raw microseismic data and have carried out a simple discrete-fracture-network (DFN) model to understand the effectiveness of the hydraulic fracturing within the study area. We have found similar observations such as the Raterman et al. (2017) study. Moving away from the wellbore, it is observed that the microseismic event count has decreased, which indicates less fracture network (Figure 4). The DFN model is generated using geologic, geomechanical, drilling, and completion data (Figure 5a and 5b). This model indicates that wider fractures

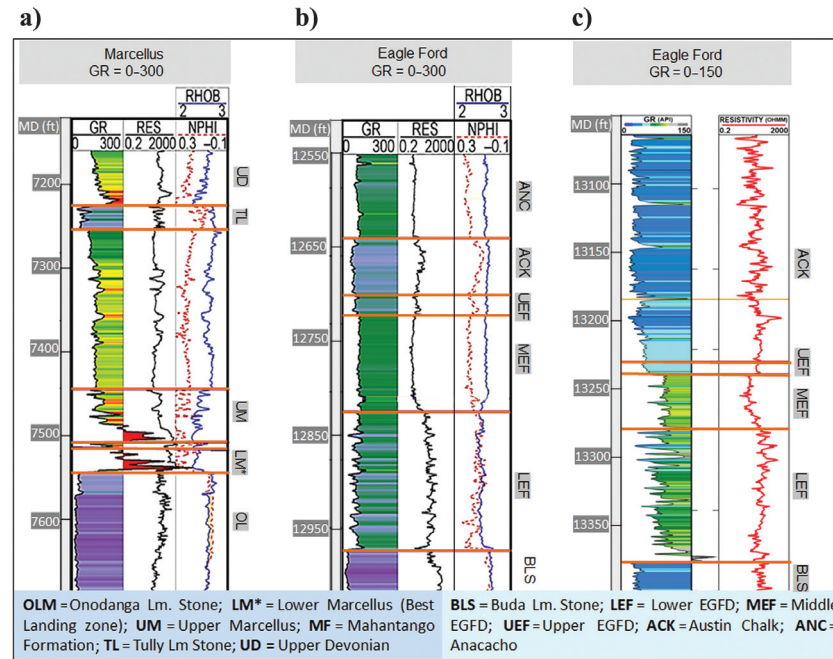


Figure 3. (a) Type log of Marcellus showing the best landing zone within lower Marcellus differentiated by high gamma. (b) Type log of Eagle Ford not showing any typical gamma log signature which can be useful in demarcating the best landing zone. (c) Eagle Ford type log with different GR scale to enhance the high gamma zone (modified from Tinnin et al., 2013; Smyer et al., 2019).

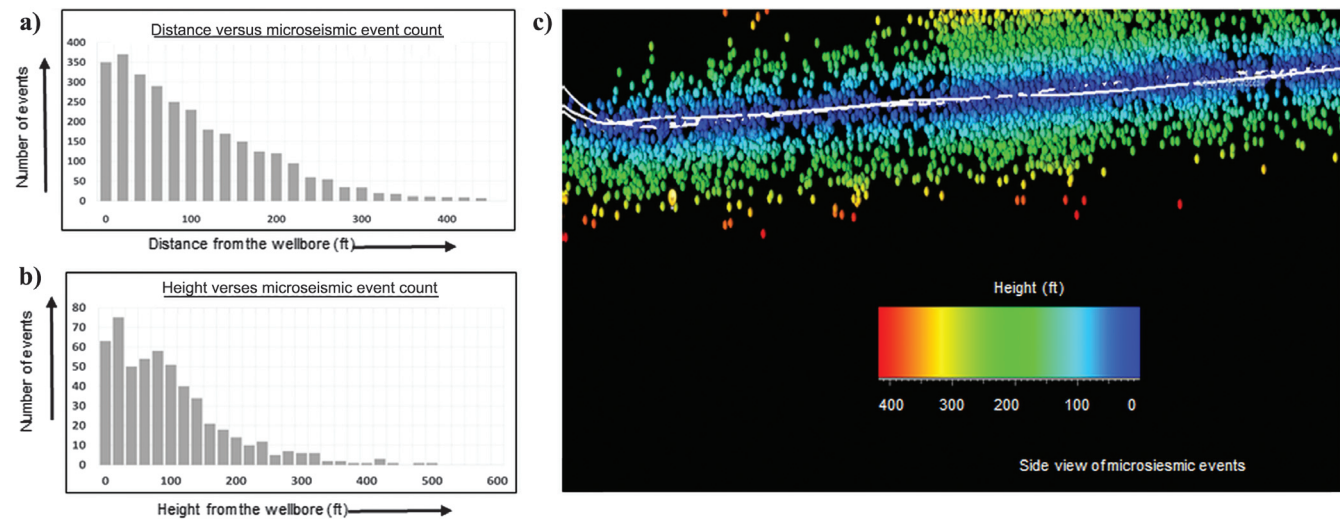


Figure 4. Maximum microseismic event concentration near the wellbore and an outer ward decreasing trend indicate effective fracturing limited around the wellbore.

happen near the wellbore, and the fractures get narrower on moving outward (Figure 5c). Proppant concentration also shows a similar kind of pattern; higher concentrations near the wellbore and a decrease away from the wellbore (Figure 5d). Conductivity plot is showing better conductivity near the wellbore (Figure 5e).

Microseismic data and the hydraulic fracture model indicate that effective fracturing takes place near the wellbore, and the maximum hydrocarbon contribution may come from the reservoir around the wellbore because of its very low inherent permeability. Thus, it becomes very crucial to identify the best zone (hydrocarbon rich and brittle) of the shale reservoir and place the lateral within the same to produce the maximum amount of hydrocarbon.

Data used for stratigraphic characterization

The first objective of the study is to understand which stratigraphic portion of the Eagle Ford shale has the favorable reservoir quality to be called the best landing zone. Then, the second objective of the study is to understand if the inconsistent production behavior of the wells 5A and 5B has any relationship with their

lateral placement. To achieve both the objectives, an integrated workflow for stratigraphic characterization was carried out. The data used in stratigraphic characterization workflow are as follows:

Production data

The normalized 12 month cumulative production data of 101 wells are considered to build various linear regression plots to capture the geologic or reservoir drivers. The production data are normalized by dividing the 12 month cumulative production of each well by their effective lateral length.

Basic wireline logs

Basic wireline logs (gamma, density, resistivity, and spectral gamma) of 22 pilot wells are used in the study as shown with the blue and the black circles in Figure 2. The basic wireline logs of these 22 wells are used to identify the depositional or lithologic pattern within Eagle Ford. The integration of log signatures with the outcrop study has guided us to further subdivide the Eagle Ford shale into smaller stratigraphic units. Three outcrops (30–50 ft thick) near Del Rio were studied to

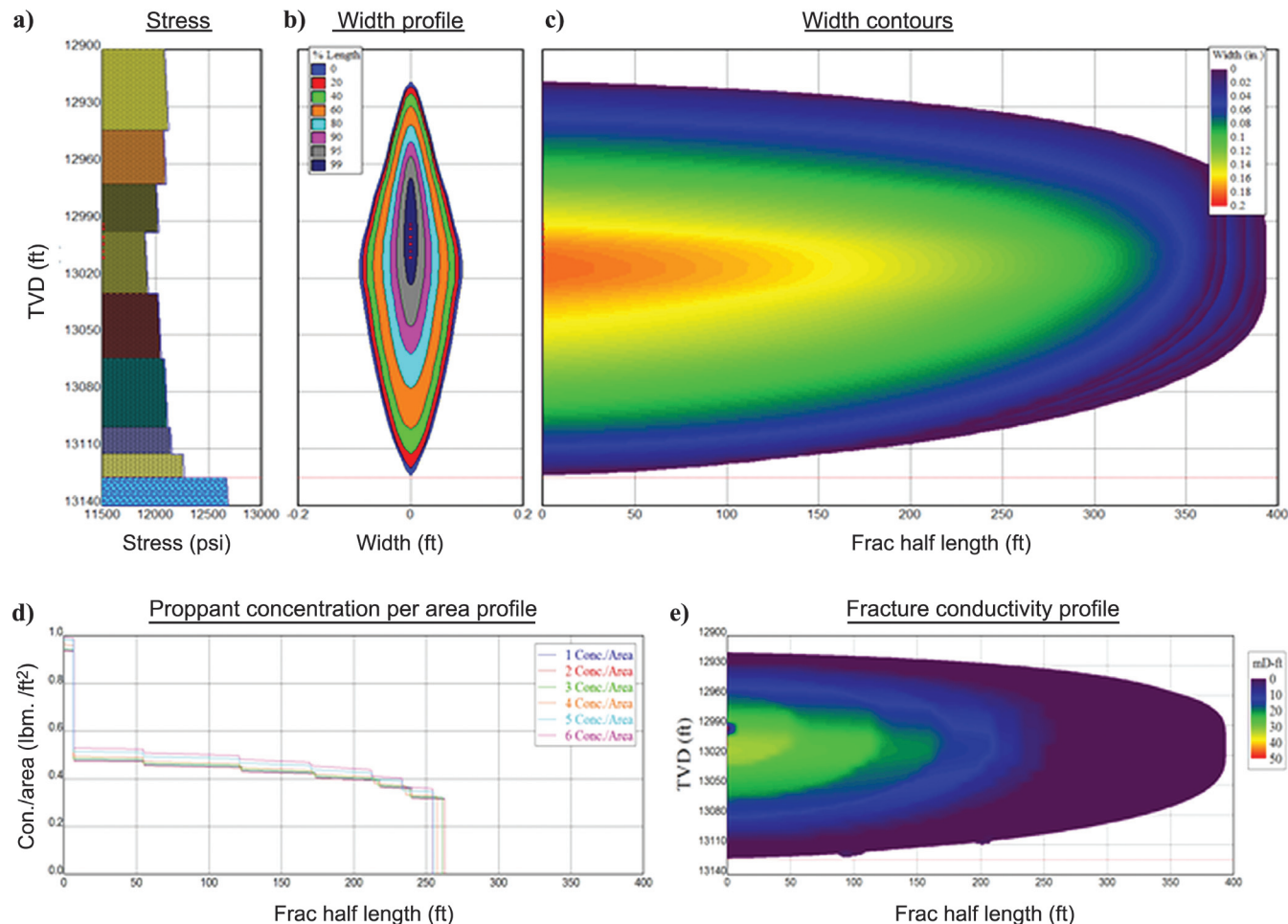


Figure 5. Hydraulic fracture model within the study area showing a decreasing trend in the effectiveness of the hydraulic fracturing constantly away from the wellbore. (a and b) The input logs, (c) the decrease trend in the width of the fractures, (d) a decreasing trend in proppant concentration, and (e) the fracture conductivity is more near the wellbore and deceases outer ward.

investigate facies stacking pattern within the exposed Eagle Ford. Detailed studies about the outcrops were given in the step 1 of workflow for stratigraphic characterization section.

Core data

There are only six wells within the study area shown with the black circles in Figure 2, which has core data sets. The core mineralogy, porosity, hydrocarbon saturation, and total organic content are used in building a multimin petrophysical model. This petrophysical model is not within the scope of this paper; however, the petrophysical model has been discussed in our earlier work ([Mukherjee et al., 2014](#)).

Processed wireline logs

Because we had only six wells having core volume of clay (Vclay), total organic carbon (TOC), porosity (PHIT), and water saturation (SWT), we processed the 22 pilot well logs using a core-log integrated petrophysical model from [Mukherjee et al. \(2014\)](#) to generate PHIT, TOC, SWT, and Vclay logs. These generated logs are then used in mapping and characterizing smaller stratigraphic units and to determine the best landing zone.

Reservoir quality maps

Based on the well-log signatures, we first mapped the top and base of the Eagle Ford shale along with the tops of nine smaller stratigraphic units within the 22 pilot wells. These tops were used in generating the depth and thickness map for smaller stratigraphic unit and the entire Eagle Ford as well. The reservoir quality (Vclay, TOC, PHIT, and SWT) maps were prepared using the processed well logs of 22 pilots. In total, six reservoir quality maps were generated within the study area. These maps are not produced in this paper due to confidentiality issue. However, we have extracted the reservoir parameters for 101 horizontal wells from these reservoir quality maps. The purpose of extracting the reservoir parameters for the horizontal wells is to generate enough data set for analytical studies (linear regression and fuzzy classification) presented in this paper.

Seismic interpreted horizons

The Eagle Ford top and base were mapped on the 3D seismic depth volume. The tops of the smaller stratigraphic units could not be mapped as they are out of seismic resolution. The seismic derived Eagle Ford base and the well top-based thickness maps of each stratigraphic unit were used to model their top surfaces through a 3D stratigraphic modeling approach.

Workflow for stratigraphic characterization

Stratigraphic characterization of the Eagle Ford shale includes subdividing the shale reservoir into fine-scale stratigraphic units and then describing them based on their reservoir parameters to identify the best among all. The identification of the best stratigraphic unit is vital

from a lateral placement point of view. The below steps are followed to subdivide the Eagle Ford into smaller stratigraphic units, characterizing the smaller units, and generate a 3D stratigraphic model.

Step 1: Divide the shale reservoir into smaller stratigraphic units

The Eagle Ford shale was divided into smaller stratigraphic zones based on the wireline log signature of subsurface wells and outcrop exposures. There are excellent outcrops, road cuts, and canyon exposures alongside and adjoining U.S. Highway 90 in Val Verde, Brewster, and Terrell Counties, Texas. These outcrops are studied by many authors and given valuable insights on the stratigraphic characteristics of the Eagle Ford shale. [Donovan et al. \(2012, 2015\)](#) describe the three outcrops of the Eagle Ford shale and produce total handheld gamma profiles for each outcrop. They subdivide the formation into five different vertical successions based on their distinct lithofacies. [Lock and Pechier \(2006\)](#) divide the Boquillas Formation (Eagle Ford equivalent) into several members representing successively transgressive, condensed, and high-stand conditions. Other works carried out on the Eagle Ford outcrops have used sedimentology ([O'Brien and Slatte, 1991](#); [Gardner et al., 2013](#)), biostratigraphy ([Van Wagoner et al., 1990](#); [Lowery and Leckie, 2017](#)), and organic geochemistry ([Miceli Romero, 2014](#)) to stratigraphically subdivide and characterize the entire Eagle Ford shale. In this paper, we investigated the depositional or lithologic pattern within the Eagle Ford shale outcrops and integrate the observations with the well-log pattern to subdivide the formation into different units over the pilot wells in the subsurface study area.

Three outcrops near Del Rio were studied to investigate the facie stacking patterns within the exposed Eagle Ford shale (Broquillas Formation) (Figure 6). The first outcrop is an impressive road cut found west of Del Rio, Texas, along the U.S. Highway 90. In this outcrop, the stratigraphic architecture of Eagle Ford was studied. This outcrop is approximately 40 ft high, and it is observed that Eagle Ford consists of small stratigraphic units of different thicknesses ranging from less than a foot to more than 2–3 ft. It also is observed that each stratigraphic unit starts with a thin layered mudstone bed and ends with a thicker carbonate-rich limestone/grainstone bed (Figure 7). The second outcrop is located at Comstock, a road cut next to the U.S. Highway 90. It was observed in this outcrop also that the Eagle Ford shale comprises smaller stratigraphic units, which show a similar kind of architecture, i.e., a thin fine-grained mudstone layer ending with a thick carbonate-rich limestone/grainstone. The thick durable limestone/grainstone beds are prominent and can be easily identified, whereas the fine-grained mudstone beds are recessive (Figure 8). The third outcrop is in Big Bend National Park of Brewster County in West Texas. In this outcrop, not only the Eagle Ford shale (Broquillas Formation) but also the underlying

Buda Limestone has been explored and studied. Again, a similar kind of stratigraphic architecture also is observed within Eagle Ford (Figure 9a).

All of the studied outcrops indicate that the Eagle Ford shale consists of smaller stratigraphic units, which are possibly related to higher-order sequence stratigraphy (Figure 9b). The smaller stratigraphic units have different thicknesses (1–3 ft), and each stratigraphic unit consists of further small layers/beds of different lithologies (ranging from few centimeters to few inches).

From the field observations, interpretation of subsurface wireline logs can be made to classify the Eagle

Ford shale into different small stratigraphic units within the subsurface study area. The Eagle Ford within the subsurface is a thick shale reservoir, reaching up to 300 ft thick. Gamma, spectral gamma, density, and deep resistivity logs are used to subdivide it into thinner stratigraphic units which range from 10 to 50 ft. The study divides the entire Eagle Ford shale reservoir into nine smaller stratigraphic units/zones (SU-1, SU-2, SU-3, SU-4, SU-5, SU-6, SU-7, SU-8, and SU-9) based on wireline log signatures (Figure 10). The upper boundary of each stratigraphic unit is defined by low gamma, high density, low resistivity, low uranium, and low thorium

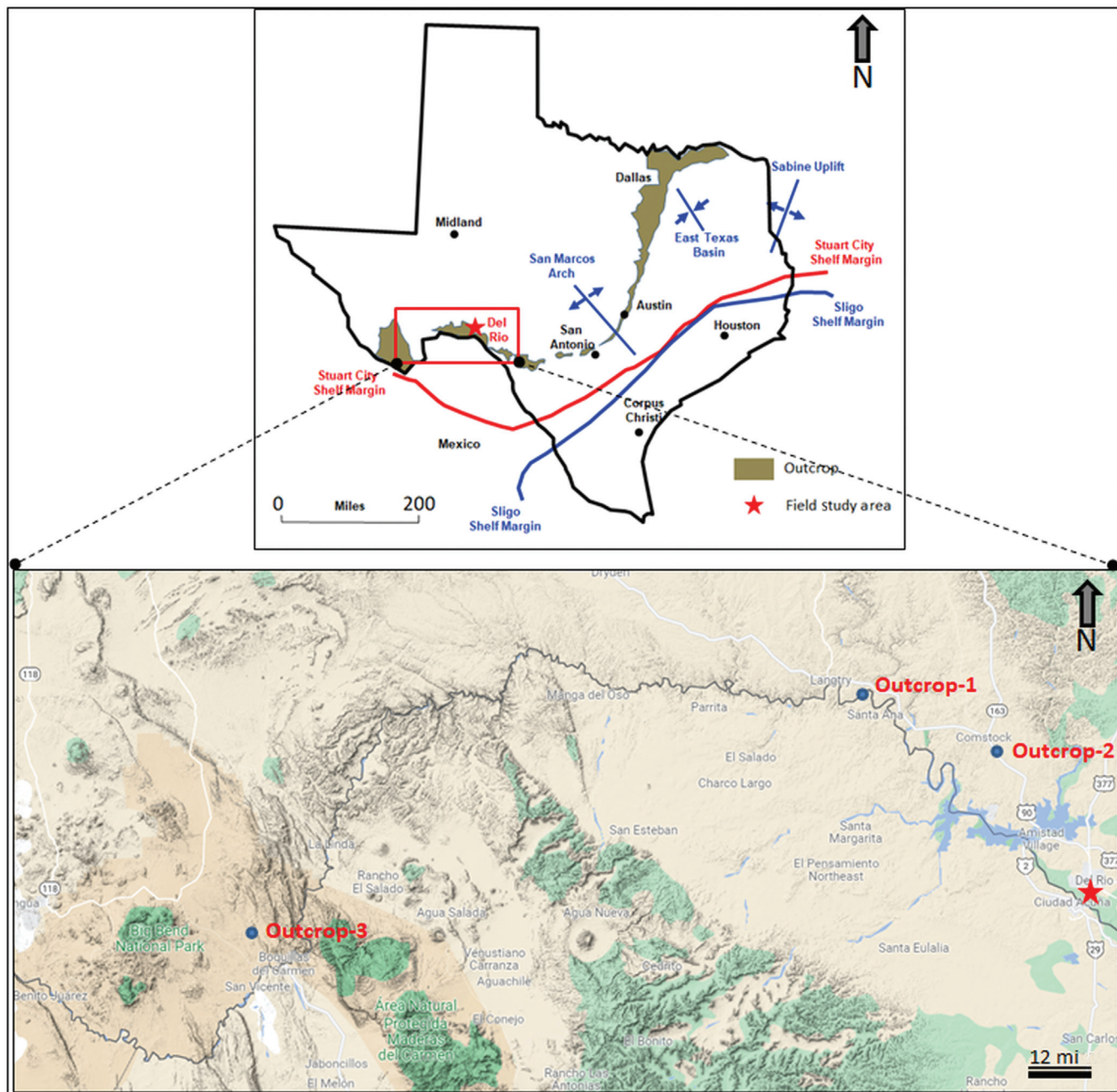


Figure 6. Map showing the outcrop of the Eagle Ford shale and the field study area near Del Rio and Big Bend National Park. Outcrop-1 near Langtry, Outcrop-2 near Comstock, and Outcrop-3 near Big Bend National Park.

log signature. Each stratigraphic unit is characterized by an upward decrease in the gamma ray, which reflects the basal mudstone coarsening up into a limestone package that is observed in the outcrops.

Step 2: Identification of key subsurface drivers

Subsurface drivers are the geologic or static reservoir parameters such as thickness, porosity, hydrocarbon saturation, total organic content, thermal maturity,

volume of clay, and reservoir pressure gradient that govern well performance. To identify the relationship between these geologic parameters and their influence on production, the first 12 months of normalized production data of the horizontal wells drilled within the study area were plotted against their average reservoir or geologic parameters (Rezaee et al., 2007; Mohaghegh, 2013; Ouenes, 2014; Roth and Royer, 2014). These reservoir parameters were derived from the reservoir attribute maps constructed from the 22 pilot well data (for more detail, see “Data used for stratigraphic characterization”). A linear regression analysis of 101 horizontal wells was carried out between the 12 month normalized production data and each geologic parameter to capture the critical geologic drivers that may influence production within the study area. The volumes of clay (Vclay), water saturation (SWT), and TOC showed the highest correlation with the normalized production data (Figure 11 and Table 2). The R -value indicates the strength of the correlation, and it can be a positive or negative value. The R -value greater than 0.8 indicates a very strong correlation, 0.8–0.6 indicates a strong correlation, 0.6–0.4 indicates a moderate correlation, and 0.4–0 indicates a weak correlation (LaMorte, 2021). Vclay is found to be the most important parameter because it shows a strongest correlation with the normalized production data, and R -value of -0.74 (Figure 11a and Table 2). Its negative correlation indicates that the production decreases with the higher volume of clay. Because the volume of clay increases, the brittleness and the pore throats of the shale decreases leading to poor production. The second important geologic parameter is the water saturation, which also has a strong correlation with normalized production having R -value of -0.7 (Figure 11b and Table 2). Higher water saturation reduces the in-place volume of hydrocarbon, thus negatively impacts the production rates. The third important parameter is TOC, which has a strong positive correlation with normalized production with and R -value of 0.6 (Figure 11c and Table 2). Along with R , low p -value (less than 0.001) and high F -stat (higher than 1) indicate that the relationships are statistically significant (Table 2). Thus, these three subsurface parameters are found to be the most crucial geologic parameters that must be controlling the

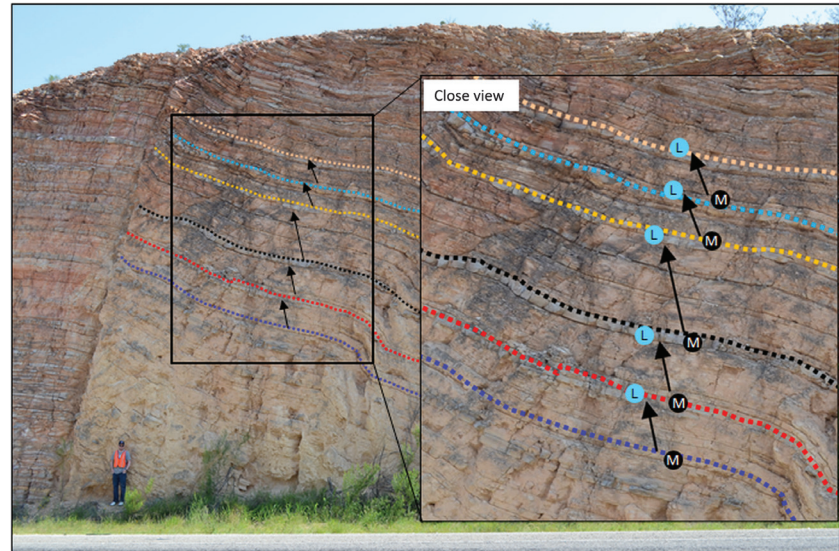


Figure 7. Road cut outcrop situated west of Del Rio, Texas, along the U.S. Highway 90, which is near Sierra Madre Oriental. The Eagle Ford shale consists of many smaller stratigraphic units (shown with the black arrows). Each stratigraphic unit shows a typical stratigraphic architecture, i.e., a thin fine-grained mudstone layer (M) at the base with gradually increasing thick carbonate-rich limestone/grainstone (L) at the top.



Figure 8. Outcrop at Comstock along the U.S. Highway 90 showing similar stratigraphic architecture within Eagle Ford shale, i.e., a thin fine-grained mudstone layer (M) at the base with gradually increasing thick carbonate-rich limestone/grainstone (L) at the top.

well productivity. Based on linear regression plots, depth and total porosity (PHIT) do not show a strong relationship with normalized production as their *R*-values are lesser than 0.6 or -0.6 within the study area. Thus, their relationship needs to be verified through some other statistical method. We have used fuzzy classification and granularity theory to crosscheck their correlation with production. On the linear regression plots, we also have observed that the total thickness of the Eagle Ford shale has a negative correlation with the production, which is against the general understanding, so we tried to address this negative correlation at the later stage of this study during validation of the workflow.

At certain times, a clear linear relationship between the subsurface parameters and the production is not obtained; thus, it becomes difficult to understand their control on the productivity of the shale. In such context, a fuzzy set and granularity theory can be applied to see if there is a relationship between the subsurface parameters and normalized production (Mohaghegh, 2013).

The fuzzy set theory allows for the representation of uncertainty, which happens either because of the random nature of events or the inaccuracy and

vagueness of the information. Fuzzy set theory is an excellent tool to understand or model uncertainty linked with ambiguity, haziness, and/or in absence of data

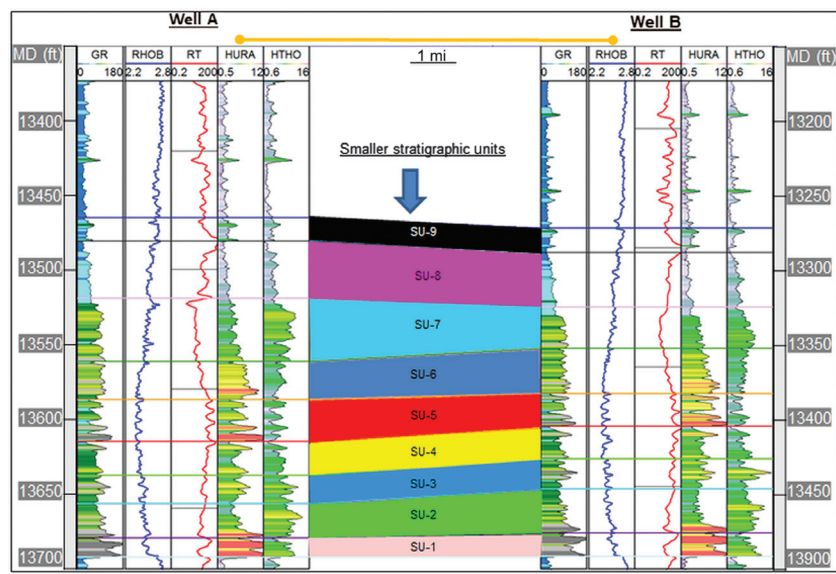


Figure 10. Nine different stratigraphic units within the shale reservoir based on wireline log data. Subdivision of the entire shale reservoir into nine smaller stratigraphic units/zones (SU-1, SU-2, SU-3, SU-4, SU-5, SU-6, SU-7, SU-8, and SU-9) based on gamma, spectral gamma, density, and deep resistivity log signatures. The upper boundary of each stratigraphic unit is characterized by low gamma, high density, low resistivity, low uranium, and low thorium. Each stratigraphic unit is characterized by an upward decrease in the gamma ray, which reflects the basal mudstone coarsening up into a limestone package.



Figure 9. (a) Outcrop in Big Bend National Park showing similar stratigraphic architecture within Eagle Ford shale, i.e., a thin fine-grained mudstone layer at the base with gradually increasing thick carbonate-rich limestone/grainstone at the top. (b) Schematic diagram showing thin beds of different gross level lithologies within the smaller stratigraphic units of Eagle Ford.

regarding a specific element of the problem at hand (Zadeh, 1965; Bezdek et al., 1984; Demirci, 1999; Baruah, 2011, 2012). For example, the low and high oil price is \$50 and \$75 per barrel, respectively. Suppose based on economics, \$60 per barrel is a cutoff between low and high for oil. If crisp sets are used to define the boundary between these prices, then \$59.99 will be grouped as a low and \$60.01 will be grouped as a high oil price. If an oil company has to take some decisions based on good and low prices, then a crisp set theory may be misleading because a crisp set reads every oil price (i.e., \$60.01, \$62, \$68, and \$72 per barrel) as high. In such a situation, grouping these prices through a fuzzy logic will be

helpful. Fuzzy logic recommends the following fuzzy sets for the price of oil. For example, an oil price of \$70 has a 15% membership for “good oil price,” whereas it has 85% membership for “high oil price” (Figure 12) (Grattan-Guinness, 1975; Deschrijver and Kerre, 2003; Mohaghegh, 2013, 2016; Mohaghegh et al., 2017; Intelligence Solution Inc., 2020). There is a concept in artificial intelligence-based data analysis, which is known as granularity. The theory of granularity helps in identifying the hidden relationship between two variables when simple regression plots do not work. The theory says that with an increase in fuzzy sets if any property shows a particular trend (increasing or decreasing) persistently, that

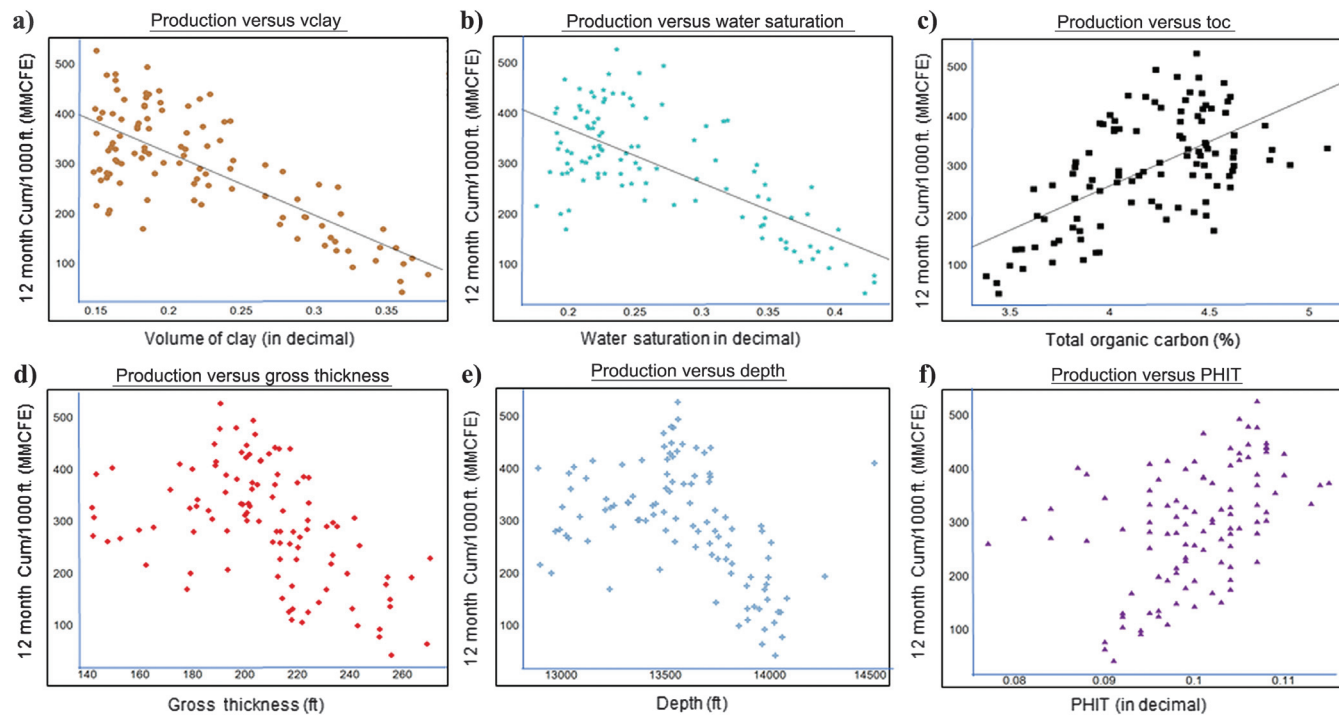


Figure 11. Crossplots between geologic/reservoir parameters and 12 month normalized cumulative production. (a and b) A strong negative linear correlation of production with Vclay and water saturation. (c) A strong positive correlation between production and TOC. (d) The gross thickness shows a weak negative correlation with production which is reverse of our general understanding. (e and f) Depth and PHIT are showing weak relationship with production based on linear regression plots, thus need to be verified through fuzzy logic and theory of granularity.

Table 2. Table showing the relationship of geologic parameters (as predictors in x-axis) with the first 12 month normalized production (as the response in y-axis).

y-axis (response)	x-axis (predictors)	p-value	F-stat	R ²	R
First 12 month cumulative production per 1000 ft lateral length (MMCFE)	Vclay	1.68E-019	125.25	0.55	-0.74
First 12 month cumulative production per 1000 ft lateral length (MMCFE)	SWT	1.55E-016	97.14	0.49	-0.70
First 12 month cumulative production per 1000 ft lateral length (MMCFE)	TOC	1.20E-011	58.28	0.36	0.60
First 12 month cumulative production per 1000 ft lateral length (MMCFE)	Gross thickness	4.83E-007	28.87	0.22	-0.47
First 12 month cumulative production per 1000 ft lateral length (MMCFE)	Depth	3.17E-006	24.30	0.19	-0.44
First 12 month cumulative production per 1000 ft lateral length (MMCFE)	PHIT	6.30E-006	22.67	0.18	0.42

Vclay, SWT, and TOC have a good relationship with production.

property has a relationship with the variable based on which the fuzzy sets are constructed. In simple words, it means that a trend is agreeable only if it remains the same at least for one level, when there is an increase in granularity. Mohaghegh (2016) and Mohaghegh et al (2017) explain the use of fuzzy set and granularity theory in determining the main drivers behind the Marcellus shale production.

The same theories were applied on the data set of the study area of Eagle Ford to find out if these theories worked similarly on a different shale play. The three parameters (depth, porosity, and thickness) were found to have a weak or unreliable correlation with normalized production based on R -values (Table 1 and Figure 11d–11f). Thickness shows a negative relationship with normalized production, which is not in line with the general understanding. Hence, it requires more insight which is explained in the “Validation of results” section. However, the fuzzy set and granularity theory were applied to depth and porosity to find out if they had any relationship with well performance. Initially, all of the wells were classified into three sets: poor, average, and good. Later, the granularity of the classifications was increased from three to four and then to five (Figure 13). On plotting the porosity and the depth of these sets of wells, a specific trend was found in the case of porosity (Figure 14a), whereas the depth did not show any trend (Figure 14b). These plots indicate that the porosity has an influence on

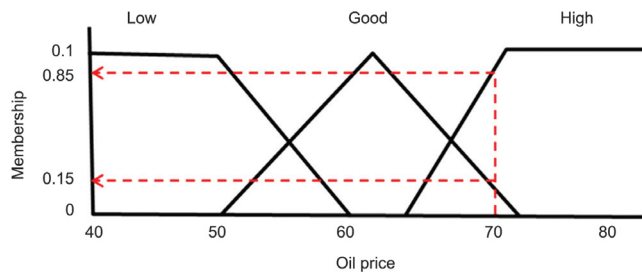


Figure 12. Fuzzy sets giving a better sense in terms of their classes. For example, an oil price 20\$ has a 15% membership for good oil price, whereas it has 85% membership for high oil price (Source: Modified after Intelligence Solution Inc.).

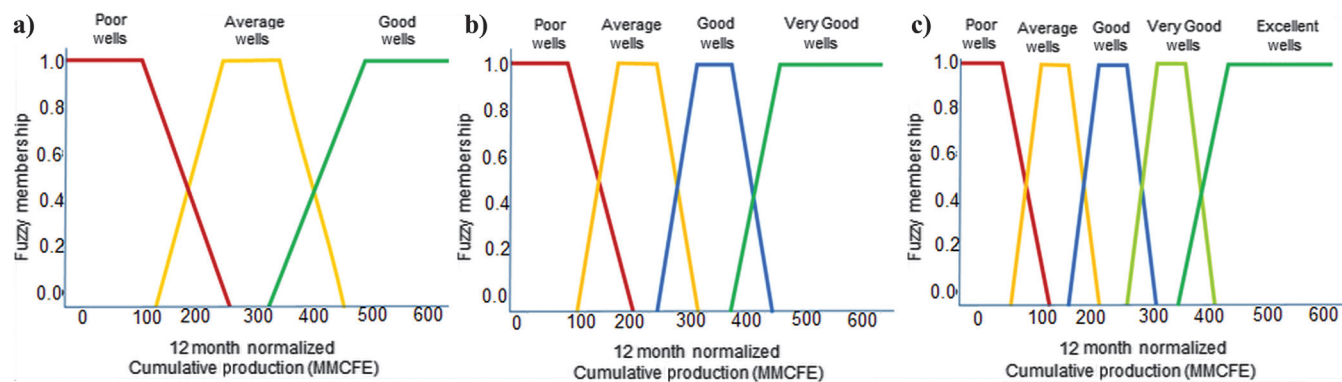


Figure 13. Fuzzy classification of the wells based on a 12 month normalized cumulative production to three, four, and five fuzzy classes.

a 12 month normalized cumulative production, but depth has low impact on production.

Linear regression has captured Vclay, TOC, and SWT, whereas fuzzy and granularity theory captured PHIT as the important geologic parameters those trend with the 12 month cumulative production. Therefore, these four parameters are considered as critical subsurface drivers. To make it a little simpler, PHIT and SWT were combined as hydrocarbon filled porosity (HCFP) using equation 1:

$$\text{HCFP} = \text{PHIT} * (1 - \text{SWT}). \quad (1)$$

Finally, the nine identified smaller stratigraphic units were characterized based on the three critical subsurface drivers (Vclay, TOC, and HCFP). A linear crossplot between normalized production and HCFP, and the related fuzzy groups indicate a strong correlation of HCFP with production (Figure 15a and 15b).

With the given data set, we did not observe a strong relationship between depth and 12 month normalized production on the crossplot (Figure 11e). The poor performance of the deeper wells shown with small production bubbles in Figure 2 is due to high volume of clay. Schieber et al. (2016), Ko et al. (2017), Reed (2017), and Gherabati et al (2016) highlight the interrelationship among depth, PHIT, pressure, thermal maturity, and production. With depth, the thermal maturity, reservoir pressure of Eagle Ford increases. Although the matrix porosity decreases with the depth, the organic porosity increases. More organic porosity is attributed to the conversion of TOC to hydrocarbon because the thermal maturity goes up (Gherabati et al., 2016; Schieber et al., 2016; Ko et al., 2017; Reed, 2017). Thus, with depth, there is a fair chance of getting favorable reservoir conditions (better maturity, high reservoir pressure, and more organic porosity), which may lead to better production. It is important to review the relationship of different geologic parameters and how it might relate to production if data are available.

Step 3: Characterization of smaller stratigraphic units

Characterization of stratigraphic units is required to identify the best vertical section in terms of reservoir

quality. Characterization is performed on the pilot wells based on Vclay, HCFP, and TOC derived from multimin processed wireline logs. It was found that the four

stratigraphic units (SU-3, 4, 5, and 6) are better than the other five units (SU-1, 2, 7, 8, and 9) in terms of higher HCFP, TOC, and low Vclay (Figure 16).

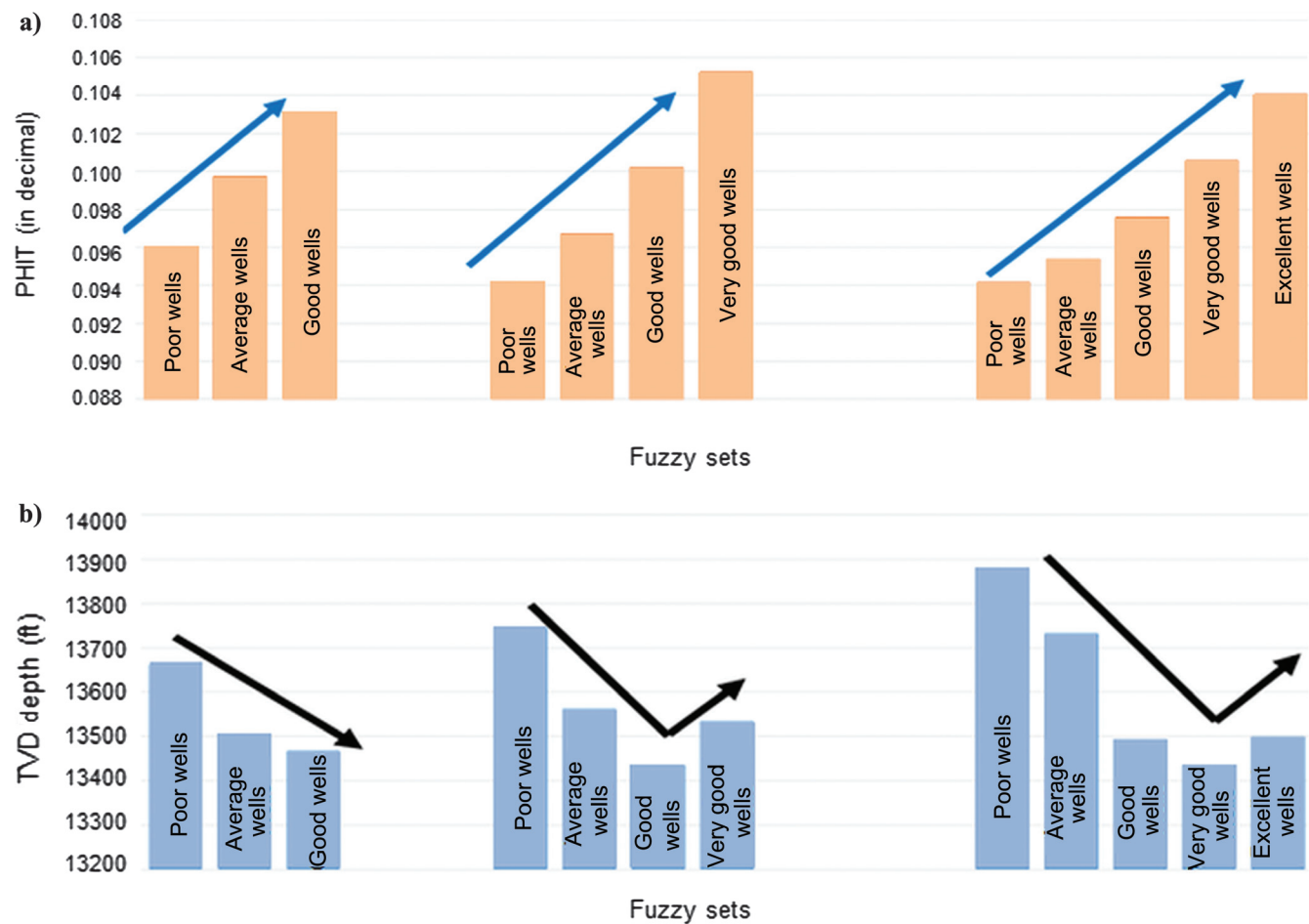


Figure 14. (a) The relationship between porosity and normalized 12 month cumulative production shows a consistently increasing trend with an increased level of granularity. It indicates that the porosity influences 12 month cumulative production. (b) The relationship between normalized 12 month cumulative production and reservoir depth does not show any trend with an increase in the level of granularity. It indicates that the depth of the shale reservoir does not influence a 12 month cumulative production in the study area.

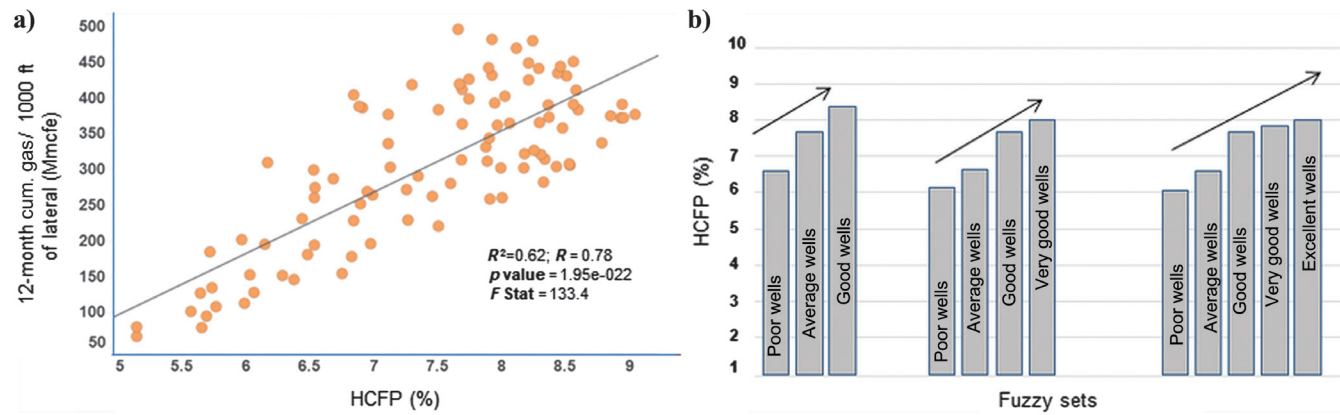


Figure 15. (a) The strong relationship with $R = 0.78$ between HCFP and normalized 12 month cumulative production as shown on the linear regression plot. (b) Fuzzy groups show a consistently increasing trend with an increased level of granularity. Both the plots suggest that there is strong correlation between HCFP and production.

The sum thickness of these four better stratigraphic units varies from 70 to 170 ft, which is a big window for effective lateral placement. To be more specific and to choose the best out of the four better stratigraphic units, it is essential to understand the heterogeneity or the range of uncertainty within the shale reservoir. The statistical measures often used to describe uncertainty are like the measures conveyed in graphical devices such as the histogram and box plot (Potter et al., 2010; Potter, 2012; Grammar and Workman, 2013; Whittaker et al., 2013; Raj et al., 2017). In this study, the box plot has been used to review the heterogeneity or the range of uncertainty of the most critical subsurface drivers within the study area. The Vclay of SU-4 and 5 ranges from 11% to 18%, whereas it ranges from 12% to 30% for SU-3 and 6 (Figure 17). Similarly, HCFP of SU-4 and 5 spreads from 6.9% to 8.9%, whereas it is 5.1%–8.7% for SU-3 and 6 (Figure 17). The TOC ranges from 8.4% to 10.8% for SU-4 and 5, whereas it is 7.3%–9.7% for SU-3 and 6 (Figure 17). The spread (first quartile to the third quartile) of Vclay, HCFP, and TOC for units 4 and 5 is lower, which indicates that these two units have lesser heterogeneity and derisks the units as a targetable reservoir. Thus, these two units (SU-4 and 5) were chosen as the best stratigraphic units and were considered together as the best landing zone.

Step 4: 3D stratigraphic model

The above steps have enabled us to subdivide the Eagle Ford Formation into smaller stratigraphic units and characterize them to identify the best landing zone within the pilot wells only. Because our objective is to review the lateral placement of two wells (5A and 5B) with regard to the best landing zone, a 3D stratigraphic model was generated. We used Eagle Ford top and base horizons mapped on seismic, seismic faults and well-based isopach maps of different stratigraphic units to build a 3D stratigraphic model with the help of PETREL modeling software. Initially, a structural framework was generated using the faults and Eagle Ford top and base seismic surfaces. Then, the top surfaces of each smaller stratigraphic unit are modeled conformably above the base of the Eagle Ford using the well-based thickness maps of each stratigraphic unit. We have graphically indicated the workflow in Figure 18.

Validation of results

Stratigraphic units 4 and 5 were identified to have the best reservoir charac-

teristics when comparing numerous geologic parameters with production (Figures 11, 16, and 17). The total thickness of the Eagle Ford had a negative trend with production (Figure 19a); however, when only considering the best stratigraphic units, a positive correlation is observed between reservoir thickness and normalized 12 month normalize production (Figure 19b and Table 3). This positive correlation suggests that the suggested workflow presented in this study can provide insight on identifying the best landing zone.

Discussion

To understand the inconsistent production behavior of the wells 5A and 5B, the lateral placements of these wells were reviewed. Although there is vertical variation of geologic parameters between the nine stratigraphic units, little laterally variability is interpreted

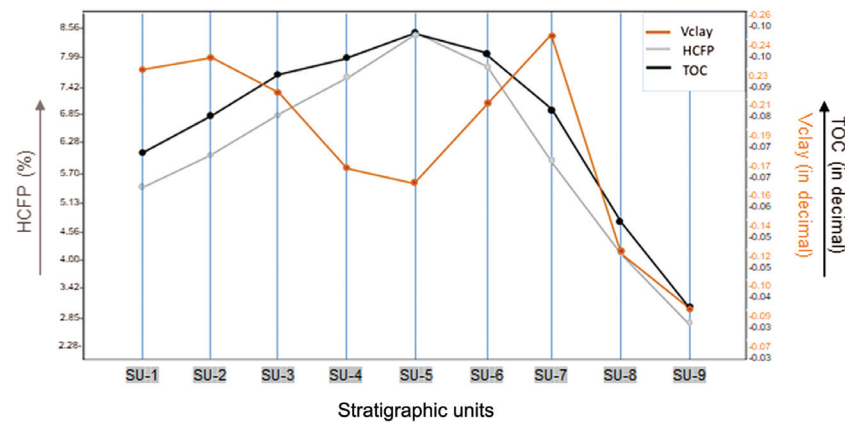


Figure 16. Histogram shows the reservoir quality of the nine stratigraphic units. SU-3, SU-4, SU-5, and SU-6 are identified as better stratigraphic units as they have comparatively higher HCFP, higher TOC, and lower Vclay with regard to other stratigraphic units.

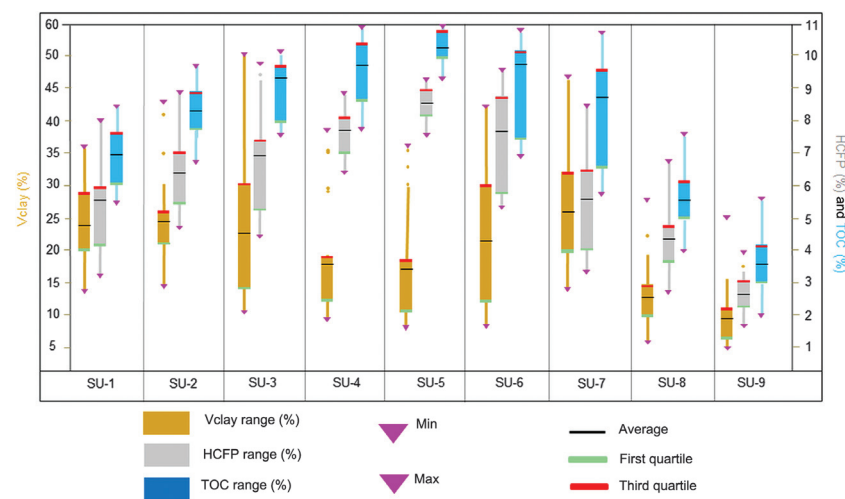


Figure 17. Box plot showing the spread of Vclay, HCFP, and TOC within each stratigraphic unit. Higher the spread, higher is the level of uncertainty. This plot shows lesser spread in Vclay, HCFP, and TOC of SU-4 and SU-5 than SU-3 and SU-6. Thus, SU-4 and SU-5 are selected as the best units out of the four better units identified in Figure 16.

to occur within each stratigraphic unit, resulting in a similar expected geology for wells 5A and 5B. The completion designs and the choke size of both the horizontal wells were similar (Table 1). Because the geology

and completion designs were similar, a similar kind of performance was anticipated. However, the normalized 12 month cumulative production of well 5B (418 MMCFGE) is much higher than that of well 5A

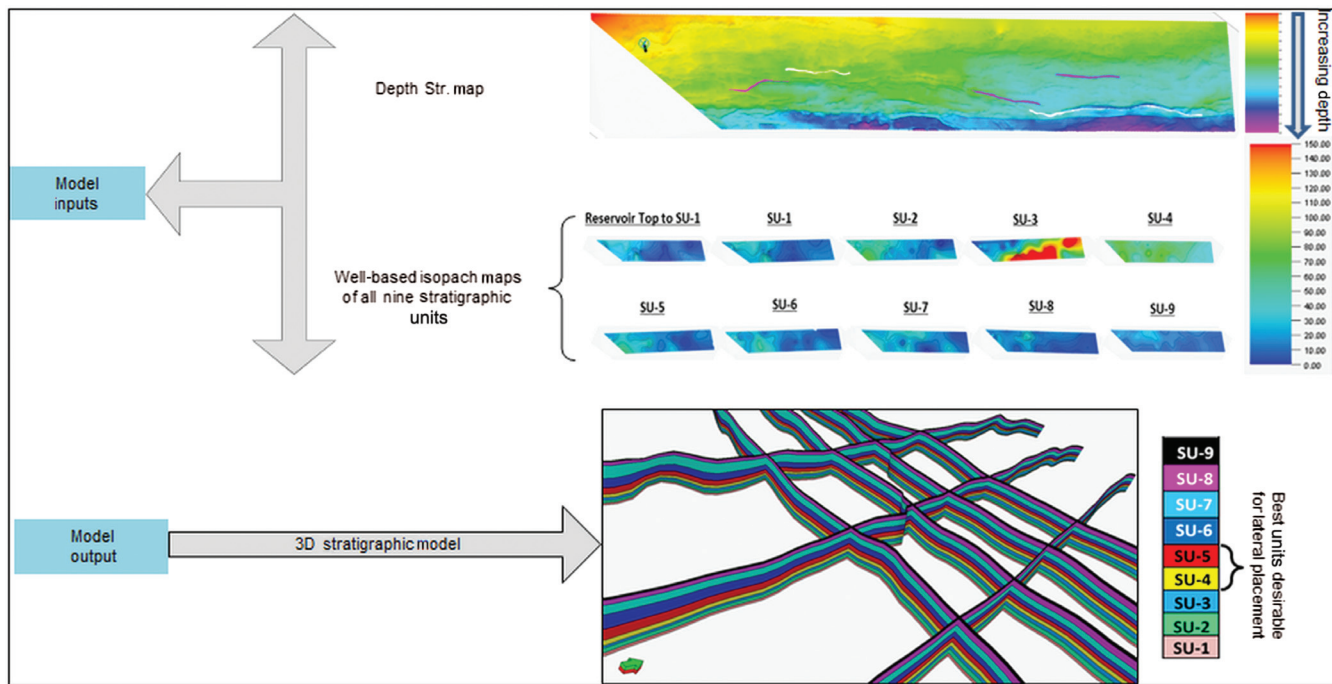
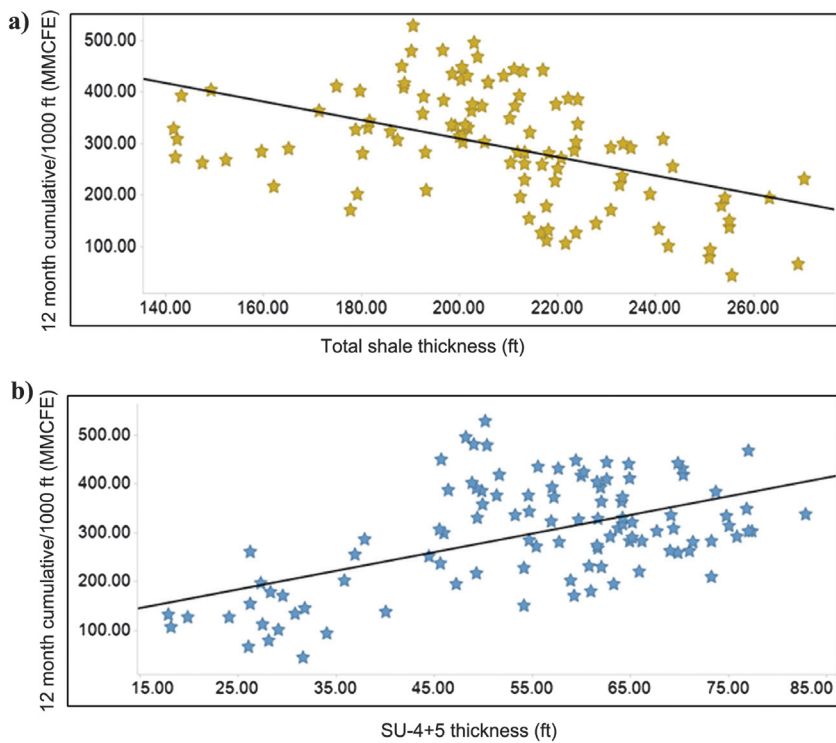


Figure 18. Input data for the 3D stratigraphic modeling and the resulted stratigraphic framework. This stratigraphic framework is generated to review the lateral placement of the two wells 5A and 5B with respect to the best stratigraphic units.

Figure 19. (a) Total shale thickness has an unrealistic negative relationship with production. (b) Sum thickness of the best stratigraphic units has a realistic positive relationship with production. This validates the workflow for identifying the best stratigraphic units. The p -value, F -stat, R^2 , and R related to both the correlations are provided in Table 3.



(262 MMCFGE). On reviewing their lateral placement with regard to the above identified best stratigraphic units (best landing zone), it was observed that the lateral placement of well 5A is only 20% within the desired units (i.e., SU-4 and 5), whereas well 5B is placed 95% within the desired units (Figure 20). Hence, we concluded that the performance difference between wells 5A and 5B is most likely due to the difference in lateral placement with regard to the best stratigraphic units. To make the conclusion of this study stronger, we tried to check this impact of lateral placement on production over some other pair of wells. Wells 5C and 5D located 500 ft away from each other and completed in the same month with similar completion design (Figure 2 and Table 4) are identified. The 12 month normalized cumulative productions of wells 5C and 5D are 443 MMCFGE and 287 MMCFGE, respectively. When the lateral placement of these two wells are reviewed, it is observed that the better producing well (5C) is placed 100% within the best landing zone, whereas the well 5D is approximately 15% within the desired zone (Figure 21). This example has strengthened our studies and observations.

Table 4. Comparison of geologic and completion parameters between wells 5C and 5D.

Parameters	Well 5C	Well 5D
Gross geologic parameters for Eagle Ford		
Depth (TVDSS-ft)	13,010	12,950
Gross thickness (ft)	225	227
TOC (wt%)	4.3	4.0
HCFP (%)	8.3	8.2
Vclay (%)	19	18
Major completion parameters		
Stage spacing (ft)	350	350
Cluster spacing (ft)	70	70
Proppant type	20/40 White Sand 30/50 White Sand	20/40 White Sand 30/50 White Sand
Proppant volume (pounds/ft)	1126	1188
Average BPM	75	76
Fluid volume (barrels/ft)	22.9	23.09
Choke size	11/64 in	11/64 in

Table 3. Table showing the relationship of the different types of thickness (as predictors in x-axis) with the first 12 month normalized production (as response in y-axis).

y-axis (response)	x-axis (predictors)	p-value	F-stat	R ²	R
First 12 month cumulative production per 1000 ft lateral length (MMCFE)	Total thickness	4.83E-007	28.87	0.22	-0.47
First 12 month cumulative production per 1000 ft lateral length (MMCFE)	Thickness of SU4 + SU5	2.38E-009	42.82	0.39	0.54

The thickness of the best stratigraphic units (SU-4 and SU-5) has realistic relationship with production validating the workflow to identify the best stratigraphic zone.

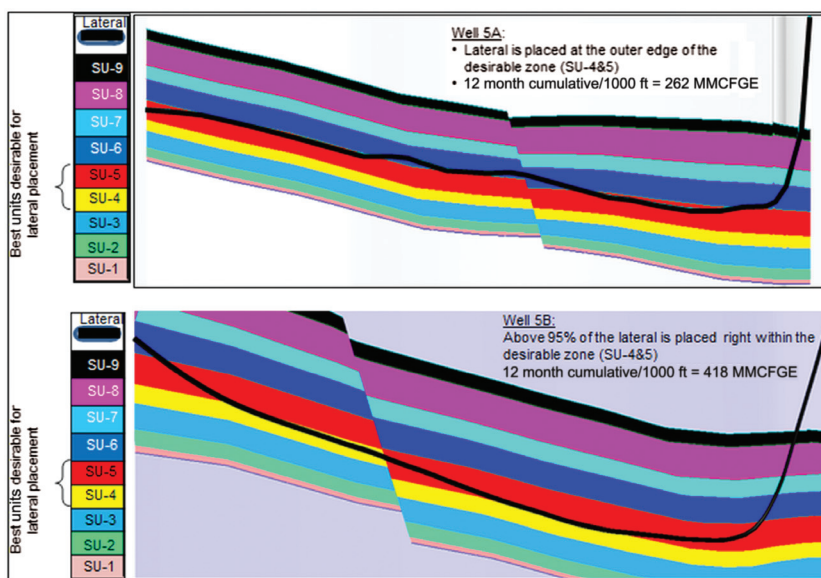


Figure 20. Cross sectional view of wells 5A and 5B generated from the 3D stratigraphic model showing the lateral placement of wells 5A and 5B with regard to the best stratigraphic units (i.e., SU-4 and 5). Approximately 95% of well 5B is placed within the best stratigraphic units, thus probably producing better than well 5A.

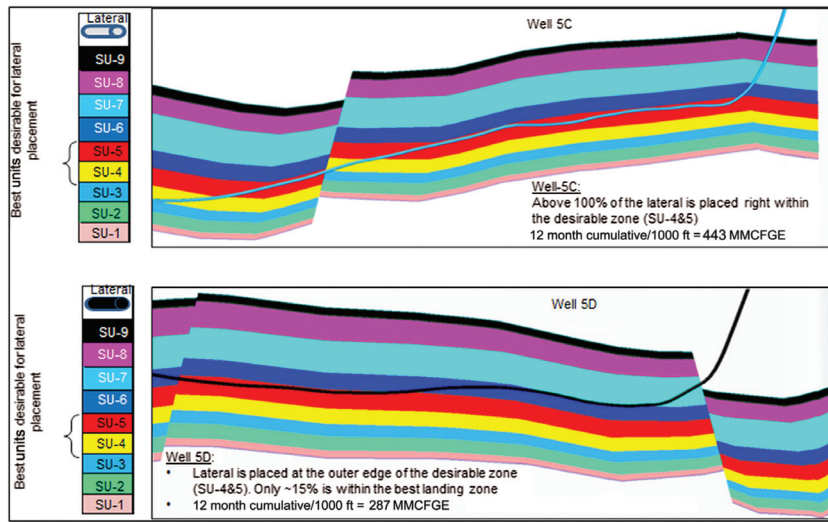


Figure 21. Cross sectional view of wells 5C and 5D generated from the 3D stratigraphic model showing the lateral placement of wells 5C and 5D with regard to the best stratigraphic units (i.e., SU-4 and 5). Approximately 100% of well 5C is placed within the best stratigraphic units, thus probably producing better than well 5D.

Conclusion

In this study, we established a semianalytical workflow for stratigraphic characterization. This stratigraphic characterization has helped us to identify the best stratigraphic units within the Eagle Ford shale. Stratigraphic units 4 and 5 are found to be the best, which have higher HCFP (7.5%–8.2%), higher TOC (9.5%–10%), and lower Vclay (17%–18%). Because of these excellent reservoir qualities, the SU-4 and SU-5 are identified as the best landing zone within the study area. The inconsistent production behavior of two closely spaced wells (5A and 5B) is found to be due to the difference in their lateral placement. The better producing well (5B with 418 MMCFGE normalized production) is placed approximately 95% within the best landing zone, whereas the lateral of well 5A is going out of the zone leading to poor performance (262 MMCFGE). This observation is verified over another set of wells (5C and 5D).

The workflow of stratigraphic characterization includes the following four steps: (1) division of shale reservoir into smaller stratigraphic units based on well logs and outcrop exposures, (2) identification of key subsurface drivers using statistical methods, (3) characterization of smaller stratigraphic units based on the key subsurface drivers, and (4) stratigraphic modeling to generate a 3D stratigraphic framework. This workflow may be useful, mainly for shale reservoirs where there are no typical log signatures (abnormal high gamma) to identify the best landing zone, unlike the Marcellus shale. This simple concept and workflow can be used by any operators in the initial phase of their development to maximize the well production. Because hundreds and thousands of wells are drilled in shale plays during their development phase, the use of this workflow may help to progress with a right strategy to avoid drilling poor wells.

Acknowledgment

The authors are thankful to Reliance Industries Ltd. for supporting the study.

Data and materials availability

Data associated with this research are confidential and cannot be released.

References

- Algarhy, A. A., R. M. Bateman, Y. Soliman, and W. Affify, 2015, An innovative technique to grade and scale shale sweet spots: North Africa Technical Conference and Exhibition, SPE, Extended Abstracts, 175854.
- Baruah, H. K., 2011, The theory of fuzzy sets: Beliefs and realities: International Journal of Energy, Information and Communications, **2**, 1–22.
- Baruah, H. K., 2012, An introduction to the theory of imprecise sets: The mathematics of partial presence: International Journal of Computational and Mathematical Sciences, **2**, 110–124.
- Bezdek, J. C., R. Ehrlich, and W. Full, 1984, FCM: The fuzzy c-means clustering algorithm: Computers & Geosciences, **10**, 191–203, doi: [10.1016/0098-3004\(84\)90020-7](https://doi.org/10.1016/0098-3004(84)90020-7).
- Cipolla, C. L., N. R. Warpinski, M. J. Mayerhofer, E. Lolon, and M. C. Vincent, 2008, The relationship between fracture complexity, reservoir properties, and fracture treatment design: Presented at the Annual Technical Conference and Exhibition, SPE, Extended Abstracts, 175854.
- David, J., R. Malpani, C. Edwards, S. Yen Han, J. Chee, L. Kok, and C. W. Wheeler, 2010, Unlocking the shale mystery: How lateral measurements and well placement impact completions and resultant production: Tight Gas Completions Conference, SPE, Extended Abstracts, 138427.
- Demirci, M., 1999, Genuine sets: Fuzzy Sets and Systems, **105**, 377–384, doi: [10.1016/S0165-0114\(97\)00235-2](https://doi.org/10.1016/S0165-0114(97)00235-2).
- Deschrijver, G., and E. E. Kerre, 2003, On the relationship between some extensions of fuzzy set theory: Fuzzy Sets and Systems, **133**, 227–235, doi: [10.1016/S0165-0114\(02\)00127-6](https://doi.org/10.1016/S0165-0114(02)00127-6).
- Donovan, A. D., T. S. Staerker, R. D. Gardner, M. C. Pope, and M. Wehner, 2015, Making outcrops relevant to the subsurface: Learnings from the Eagle Ford Group in West Texas: Unconventional Resources Technology Conference, SPE/SEG/AAPG, Extended Abstracts, 2154599.
- Donovan, A. D., T. S. Staerker, A. Pramudito, W. Li, M. J. Corbett, C. M. Lowery, A. M. Romero, and R. D. Gardner, 2012, The Eagle Ford outcrops of West Texas: A field laboratory for understanding heterogeneities within unconventional mudstone reservoirs: Gulf Coast Association of Geological Societies, **1**, 162–185.

- Dutta, J., A. K. Sahoo, and M. Srivastava, 2018, 3D pore pressure modeling of a shale gas reservoir and its implication: 4th South Asian Geosciences Conference and Exhibition, Association of Petroleum Geologist, Extended Abstracts, AU448.
- Dutta, J., A. K. Sahoo, V. Vishal, and M. Srivastava, 2019, Effect of fluid expansion and clay diagenesis on shale reservoirs: Oil and Gas India Conference and Exhibition, SPE, Extended Abstracts, 194657.
- El Sgher, M., A. Kashy, and S. Ameri, 2021, Evaluation of hydraulic fracturing treatment with microseismic data analysis in a Marcellus shale horizontal well: Western Regional Meeting, SPE, Extended Abstracts, 200877.
- Eslinger, E., 2007, Procedures for lithology characterization and probabilistic up-scaling (curve “blocking”) using petrophysical and core data: AAPG Annual Convention, AAPG Search and Discovery, Extended Abstracts, 90063.
- Gardner, R. D., M. C. Pope, M. P. Wehner, and A. D. Donovan, 2013, Comparative stratigraphy of the Eagle Ford Group strata in Lozier Canyon and Antonio Creek, Terrell County, Texas: Transactions-Gulf Coast Association of Geological Societies, **63**, 673–674.
- Gherabati, S., J. Browning, F. Male, S. Ikonnikova, and G. McDaid, 2016, The impact of pressure and fluid property variation on well performance of liquid-rich Eagle Ford shale: Journal of Natural Gas Science and Engineering, **33**, 1056–1068, doi: [10.1016/j.jngse.2016.06.019](https://doi.org/10.1016/j.jngse.2016.06.019).
- Grammer, G. M., and S. Workman, 2013, Integrating depositional facies and sequence stratigraphy in characterizing unconventional reservoirs: Eagle Ford Shale, South Texas: Gulf Coast Association of Geological Societies Transactions, **63**, 473–508.
- Grattan-Guinness, I., 1975, Fuzzy membership mapped onto interval and many-valued quantities: Mathematical Logic Quarterly, **22**, 149–160, doi: [10.1002/malq.19760220120](https://doi.org/10.1002/malq.19760220120).
- Gupta, M., P. Jain, A. Shrivastava, M. Srivastava, and B. Deka, 2016, Role of multivariate analysis to define the key driver's governing the well productivity in Marcellus shale: Unconventional Resources Technology Conference, SPE/SEG/AAPG, Extended Abstracts, 2460969.
- Hazra, B., D. A. Wood, V. Vishal, and A. K. Singh, 2018a, Pore characteristics of distinct thermally mature shales: Influence of particle size on low-pressure CO₂ and N₂ adsorption: Energy & Fuels, **32**, 8175–8186, doi: [10.1021/acs.energyfuels.8b01439](https://doi.org/10.1021/acs.energyfuels.8b01439).
- Hazra, B., D. A. Wood, V. Vishal, A. K. Varma, D. Sakha, and A. K. Singh, 2018b, Porosity controls and fractal disposition of organic-rich Permian shales using low-pressure adsorption techniques: Fuel, **220**, 837–848, doi: [10.1016/j.fuel.2018.02.023](https://doi.org/10.1016/j.fuel.2018.02.023).
- Hentz, T., and S. Ruppel, 2011, Regional stratigraphic and rock characteristics of Eagle Ford Shale in its play area: Maverick Basin to East: AAPG Annual Convention and Exhibition, AAPG, 10325.
- Shale Analytics, 2020, Intelligent Solutions, Inc., www.IntelligentSolutionsInc.com, accessed 21 July 2020.
- Kampfer, G., and M. Dawson, 2016, A novel approach to mapping hydraulic fractures using poromechanics principles: 50th U.S. Rock Mechanics/Geomechanics Symposium, ARMA, Extended Abstracts, 2016-843.
- Ko, L. T., R. G. Loucks, S. C. Ruppel, T. Zhang, and S. Peng, 2017, Origin and characterization of Eagle Ford pore networks in the South Texas Upper Cretaceous Shelf: AAPG Bulletin, **101**, 387–418, doi: [10.1306/08051616035](https://doi.org/10.1306/08051616035).
- LaMorte, W. W., 2021, Correlation and regression: Evaluating association between two continuous variables, <https://sphweb.bumc.bu.edu/otlt/MPH-Modules/PH717-QuantCore/PH717-Module9-Correlation-Regression/PH717-Module9-Correlation-Regression4.html>, accessed 3 September 2021.
- Lock, B. E., and L. Pechier, 2006, Boquillas (Eagle Ford) upper slope sediments, West Texas: Outcrop analogs for potential shale reservoirs: GCAGS Annual Convention, AAPG, 90056.
- Lowery, C., and M. Leckie, 2017, Biostratigraphy of the Cenomanian-Turonian Eagle Ford Shale of South Texas: The Journal of Foraminiferal Research, **47**, 105–128, doi: [10.2113/gsjfr.47.2.105](https://doi.org/10.2113/gsjfr.47.2.105).
- Lucas, W. B., D. L. Sam, G. L. Michael, and T. P. Terry, 2010, Improving production in the Eagle Ford shale with fracture modeling, increased conductivity and optimized stage and cluster spacing along the horizontal wellbore: Tight Gas Completions Conference, SPE, Extended Abstracts, 138425.
- Meyer, M. J., 2018, High-resolution chemostratigraphy of the Woodbine and Eagle Ford Groups, Brazos Basin, Texas: M.S. thesis, Texas A&M University.
- Miceli Romero, A., 2014, Subsurface and outcrop organic geochemistry of the Eagle Ford Shale (Cenomanian-Coniacian) in west, southwest, central, and east Texas: Ph.D. dissertation, University of Oklahoma.
- Mohaghegh, S. D., 2013, Reservoir modeling of shale formations: Journal of Natural Gas Science and Engineering, **12**, 22–33, doi: [10.1016/j.jngse.2013.01.003](https://doi.org/10.1016/j.jngse.2013.01.003).
- Mohaghegh, S. D., 2016, Fact-based re-frac candidate selection and design in shale — A case study in application of data analytics: Unconventional Resources Technology Conference, SPE/SEG/AAPG, Extended Abstracts, 2433427.
- Mohaghegh, S. D., R. Gaskari, and M. Maysami, 2017, Shale analytics: Making production and operational decisions based on facts: A case study in Marcellus Shale: Hydraulic Fracturing Technology Conference and Exhibition, SPE, Extended Abstracts, 184822.
- Mukherjee, D., A. Sahoo, A. Mukherjee, and M. Srivastava, 2014, Core-log integrated approach: A solution to the petrophysical characterization of the Eagle Ford Shale: Annual Convention and Exhibition, AAPG, 90189.
- O'Brien, N. R., and R. M. Slatte, 1991, Argillaceous rock atlas: Springer-Verlag.

- Ouenes, A., 2014, Distribution of well performances in shale reservoirs and their predictions using the concept of shale capacity: European Unconventional Resources Conference and Exhibition, SPE/EAGE, 167779.
- Potter, K., 2012, Uncertainty: From quantification to visualization, <http://www.sci.utah.edu/~kpotter/talks/StatisticalUncertainty.pdf>, accessed 12 September 2018.
- Potter, K., J. R. Riesenfeld, and C. R. Johnson, 2010, Visualizing summary statistics and uncertainty: Computer Graphics Forum, **29**, 823–832, doi: [10.1111/j.1467-8659.2009.01677.x](https://doi.org/10.1111/j.1467-8659.2009.01677.x).
- Raj, M., M. Mahsa, R. Robert, M. K. Robert, and R. T. Whitaker, 2017, Path boxplots: A method for characterizing uncertainty in path ensembles on a graph: Journal of Computational and Graphical Statistics, **26**, 243–252, doi: [10.1080/10618600.2016.1209115](https://doi.org/10.1080/10618600.2016.1209115).
- Raterman, K., H. Farrell, O. Mora, A. Janssen, S. Busetti, J. McEwan, B. Roy, K. Friehauf, and J. Rutherford, 2017, Sampling a stimulated rock volume: An Eagle Ford example: Unconventional Resources Technology Conference, SPE/SEG/AAPG, Extended Abstracts, 2670034.
- Reed, R., 2017, Organic-matter-pores: New findings from lower-thermal-maturity mudrocks: Gulf Coast Association of Geological Societies Journal, **6**, 99–110.
- Rezaee, R., R. M. Slatt, and R. F. Sigal, 2007, Shale gas rock properties prediction using artificial neural network technique and multi regression analysis, an example from a North American Shale gas reservoir: Australian Society of Exploration Geophysicists (ASEG) — 19th Geophysical Conference, Extended Abstracts, 1–4.
- Roth, M., and T. Royer, 2014, An analytic approach to sweet spot mapping in the Eagle Ford unconventional play: CSPG/CSEG/CWLS Geo Convention, AAPG, Extended Abstracts, 80406.
- Roussel, N. P., and S. Agrawal, 2017, Introduction to poroelastic response monitoring — Quantifying hydraulic fracture geometry and SRV permeability from offset-well pressure data: Unconventional Resources Technology Conference, SPE/SEG/AAPG, 2645414.
- Sahoo, A. K., D. Biswal, and M. Srivastava, 2015, Workflow to optimize field development strategy and maximize recovery of a shale play: Oil and Gas India Conference and Exhibition, SPE, Extended Abstracts, 178120-MS.
- Sahoo Ajit, K., A. Behera, V. Vishal, and M. Srivastava, 2018, Predict the production: A data analytic approach: 4th South Asian Geosciences Conference and Exhibition, Association of Petroleum Geologist, Extended Abstracts, AU320.
- Sahoo Ajit, K., D. Mukherjee, A. Mukherjee, and M. Srivastava, 2013, Reservoir characterization through lithofacies identification for identification of sweet spot and best landing point: Unconventional Resource Technology Conference, SPE/SEG/AAPG, Extended Abstracts, 1561817.
- Sahoo Ajit, K., R. Mukherjee, D. Mukherjee, and M. Srivastava, 2014, Application of lithofacies modeling in enhancing well productivity; an example from Eagle Ford shale: Unconventional Resource Technology Conference, SPE/SEG/AAPG, Extended Abstracts, 1921815.
- Schieber, J., R. Lazar, K. Bohacs, B. Klimentidis, J. Ottmann, and M. Dumitrescu, 2016, An SEM study of porosity in the Eagle Ford Shale of Texas — Pore types and porosity distribution in a depositional and sequence stratigraphic context, in J. A. Breyer, ed., The Eagle Ford Shale: A renaissance in U.S. oil production: AAPG 110, 167–186.
- Slatt Roger, M., P. Singh, R. P. Philp, K. J. Marfurt, Y. Abousleiman, and N. R. O'Brien, 2018, Workflow for stratigraphic characterization of unconventional gas shales, https://www.researchgate.net/profile/Roger_Slatt/publication/254528869_Workflow_for_Stratigraphic_Characterization_of_Unconventional_Gas_Shales/links/53fcfc7e0cf22f21c2f67e47/Workflow-for-Stratigraphic-Characterization-of-Unconventional-Gas-Shales.pdf, accessed 7 February 2018.
- Smyer, K. M., H. S. Hamlin, R. Eastwood, and G. McDaid, 2019, Variability of geologic properties of shale gas and tight oil plays: Gulf Coast Association of Geological Societies, **8**, 191–209.
- Stephenson, B., B. Nesheli, K. Christopher, A. Mookerejee, D. Rampton, and N. Teft, 2015, Subsurface-driven completion and well-design changes to maximize value in the Marcellus: AAPG Annual Convention and Exhibition, Extended Abstracts, 41634.
- Surles, M. A., 1987, Stratigraphy of the Eagle Ford Group (Upper Cretaceous) and its source-rock potential in the East Texas Basin: Baylor Geological Studies Bulletin, **45**, 1–57.
- Thomson, J., Z. Greg, and T. Leshchyshyn, 2016, Completion design production case study in the Duvernay Shale Formation: Presented at the Annual Technical Conference and Exhibition, SPE, Extended Abstracts, 181715.
- Tinnin, B. M., G. Hildred, and N. Martinez, 2013, Expanding the application of chemostratigraphy within Cretaceous mudrocks: Estimating total organic carbon and paleoredox facies using major, minor and trace element geochemistry: Unconventional Resource Technology Conference, SPE/AAPG/SEG, Extended Abstracts, 1579472.
- Urban-Rascon, E., C. Virues, and R. Aguilera, 2018, 3D geomechanical modeling in the complex fracture network of the Horn River shale using a fully coupled hybrid hydraulic fracture HHF model: Permeability evolution and depletion: Canada Unconventional Resources Conference, SPE, Extended Abstracts, 189795.
- U.S. Energy Information Administration, 2021, Drilling productivity report, <https://www.eia.gov/petroleum/drilling/pdf/eagleford.pdf>, accessed 6 September 2021.
- Van Wagoner, J. C., R. M. Mitchum, K. M. Campion, and V. D. Rahmanian, 1990, Siliciclastic sequence stratigraphy in well logs, cores, and outcrops: Concepts for high-resolution correlation of time and facies: AAPG, AAPG Methods in Exploration Series 7, 402–403.

- Vishal, V., D. Chandra, J. Bahadur, D. Sen, B. Hazra, B. Mahanta, and D. Mani, 2019, Interpreting pore dimensions in gas shales using a combination of SEM imaging, small-angle neutron scattering, and low-pressure gas adsorption: *Energy & Fuels*, **33**, 4835–4848, doi: [10.1021/acs.energyfuels.9b00442](https://doi.org/10.1021/acs.energyfuels.9b00442).
- Whitaker, R. T., M. Mirzargar, and R. M. Kirby, 2013, Contour boxplots: A method for characterizing uncertainty in feature sets from simulation ensembles: *IEEE Transactions on Visualization and Computer Graphics*, **19**, 2713–2722, doi: [10.1109/TVCG.2013.143](https://doi.org/10.1109/TVCG.2013.143).
- White, T., L. Gonzalez, G. Ludvigson, and C. Poulsen, 2001, Middle Cretaceous greenhouse hydrologic cycle of North America: *Geological Society of America*, **29**, 363–366.
- Workman, S., 2013, Integrating depositional facies and sequence stratigraphy in characterizing unconventional reservoirs: Eagle Ford Shale, South Texas: Western Michigan University, 1–152.
- Zadeh, L. A., 1965, Fuzzy sets: *Information and Control*, **8**, 338–353, doi: [10.1016/S0019-9958\(65\)90241-X](https://doi.org/10.1016/S0019-9958(65)90241-X).
- Zillur, R., and M. Y. Al-Qahtani, 2001, Using radioactive tracer log, production tests, fracture pressure match, and pressure transient analysis to accurately predict fracture geometry in Jauf Reservoir, Saudi Arabia: Presented at the Annual Technical Conference and Exhibition, SPE, Extended Abstracts, 71650.

Biographies and photographs of the authors are not available.